Relationship among Phase Morphology, Oil Resistance, and Thermal Aging Properties in CPE/NR Blends: Effect of Blending Conditions

Chakrit Sirisinha,[1,2] Pongdhorn Saeoui,[3] Jantagarn Guaysomboon[1]

[1]*Department of Chemistry, Faculty of Science, Mahidol University, Rama 6 Rd., Bangkok 10400, Thailand*
[2]*Center of Excellence (Rubber Research Unit), Faculty of Science, Mahidol University, Salaya Campus, Phutthamonthon 4 Rd., Salaya , Nakhon Pathom, 73170, Thailand*
[3]*The National Metal and Materials Technology Center (MTEC), Rama 6 Rd., Bangkok 10400, Thailand*

Received 18 March 2003; accepted 30 April 2003

ABSTRACT: The CPE/NR blends with blend ratio of 50/50% by weight were prepared with various blending conditions. The resistance to oil and thermal aging of the blends was investigated and correlated with phase morphology. The NR dispersed phase size in blends was found to decrease with increasing rotor speed up to 45 rpm and subsequently level off at higher rotor speeds. With increasing mixing time at a given rotor speed, NR dispersed phase size reached a minimum and increased again with a further increase in mixing time, caused by domain breakup and phase coalescence, respectively. In addition, the results revealed a strong relationship between NR phase size and resistances to oil as well as thermal aging, that is, the smaller the dispersed phase size, the higher the oil resistance and the thermal aging properties. © 2003 Wiley Periodicals, Inc. J Appl Polym Sci 90: 4038–4046, 2003

Key words: morphology

INTRODUCTION

Blending of two polymers usually gives rise to a new material having a better balance of properties than a single polymer. Blending of elastomers is undertaken for three main reasons: (1) improvement of the technical properties of the original elastomer, (2) achievement of improved processing behavior, and (3) reduction in compound cost.[1,2]

Chlorinated polyethylene (CPE) consists of ethylene units and chloroethylene units. Because of its linear backbone, lack of unsaturation, and the presence of high polarity of chlorine groups, CPE tends to be very resistant to oil, ozone, heat, flame, and nonpolar chemicals. The major applications for CPE are wire and cable coating; hose-cover and tube; sponge; sheeting, pond liners; impact modification in poly (vinyl chloride) (PVC) and acrylonitrile–butadiene–styrene copolymers (ABS).[3] Although CPE is relatively expensive, its cost can be reduced through blending with less costly rubber such as natural rubber (NR). It has been reported that CPE up to 50% by weight could be substituted by NR, giving similar tensile properties to pure CPE.[4]

Correspondence to: C. Sirisinha (sccsr@mahidol.ac.th).
Contact grant sponsors: the Thailand Graduate Institute of Science and Technology (TGIST) and National Science and Technology Development Agency (NSTDA)

Journal of Applied Polymer Science, Vol. 90, 4038–4046 (2003)

However, most polymer blends are thermodynamically immiscible because of the positive enthalpy change of mixing (ΔH) and the lower entropy change of mixing (ΔS) resulting from a high molecular weight of polymers. Blending usually leads to a heterogeneous morphology. Types of morphology and phase dimensions determine the properties of heterogeneous polymer blends.[5] To be able to control the blend properties, the morphology development should be understood. The morphology of heterogeneous polymer blends depends on the blend composition,[5–16] interfacial tension between the constituent polymers,[17–23] viscosity ratio,[20,24–29] elasticity ratio,[24,30] and processing conditions.[5,23,24,31–41] The previous work[4] shows that with NR content up to 50% by weight, oil resistance, and aging properties of CPE/NR blends are close to those of pure CPE. The present study, therefore, aims to further the previous work[4] by investigating the influences of mixing conditions on phase morphology, oil resistance, and thermal aging properties in CPE/NR blends.

EXPERIMENTAL

Materials

Chlorinated polyethylene or CPE (3615P, DuPont Dow Elastomer Co., Ltd., USA) with chlorine content of 36%, and natural rubber or NR (STR 5 Thailand, ML1+4 at 100°C = 72) were used in the present study. Dicumyl peroxide or DCP (Percumyl D, Chemmin Co., Ltd., Thailand) was used as a curing agent.

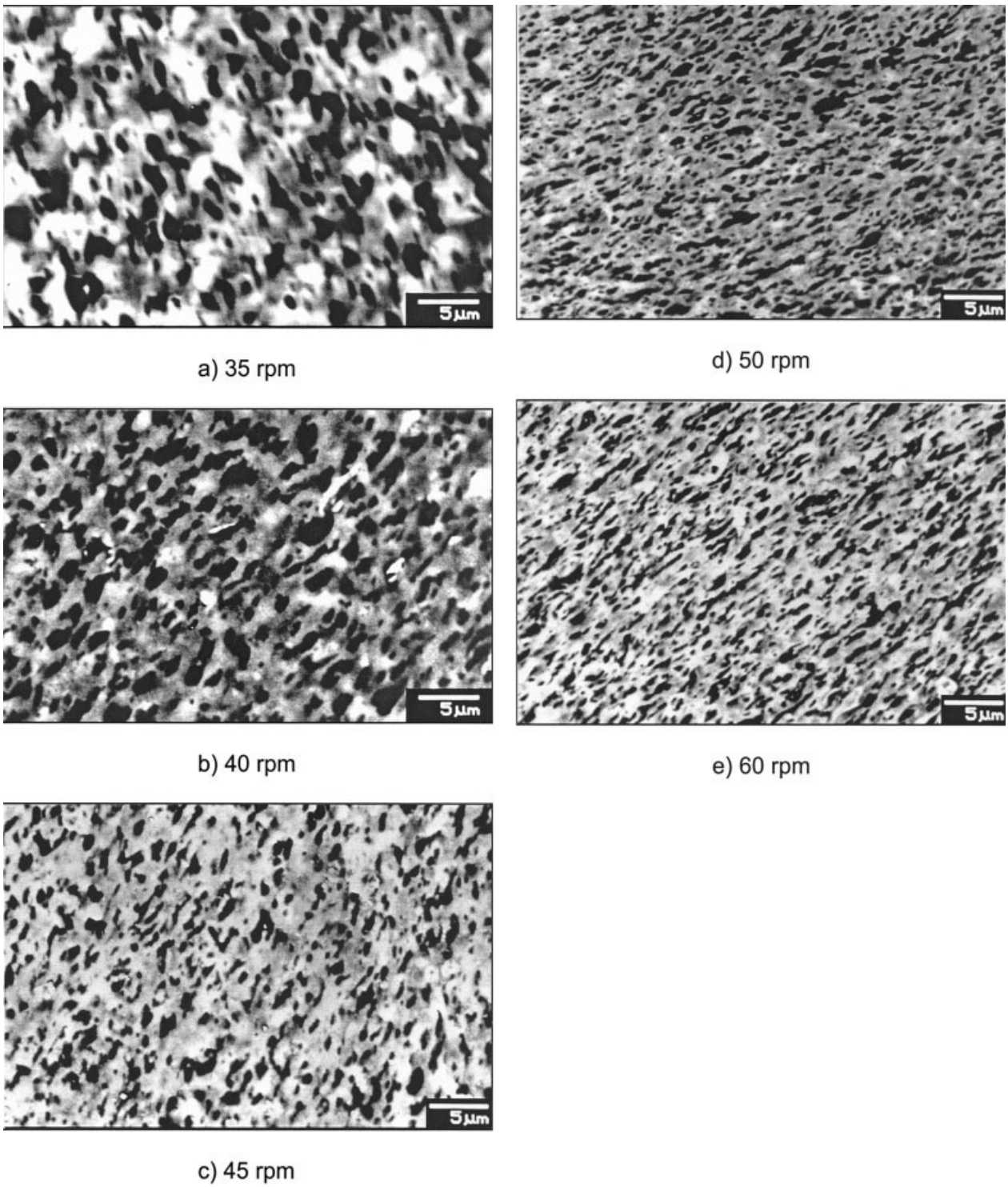

Figure 1 Scanning electron micrographs of CPE/NR blends with various rotor speeds: (a) 35 rpm; (b) 40 rpm; (c) 45 rpm; (d) 50 rpm; (e) 60 rpm.

Mixing procedure

The CPE/NR blends with the blend ratio of 50/50 were prepared by melt blending in a laboratory-size internal mixer (Haake Rheomix 90) with a fill factor of 0.6. NR was initially masticated for a minute, and CPE was then charged and mixing was carried on. One phr of DCP was added to the blends for 1 min before discharging the blends. The blends were thereafter sheeted on the cooled two-roll mill and, finally, compression molded into 2 mm-thick sheets under a pressure of 15 MPa at 155°C for 32 min (which gives about 96% cure calculated from half-life of DCP). To inves-

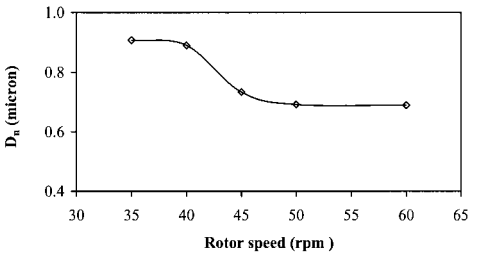

Figure 2 Relationship between dispersed phase size and rotor speed.

tigate the influences of mixing conditions, various mixing times from 5 to 7 min and rotor speeds from 35 to 60 rpm were used.

Measurements of tensile properties and hardness

Tensile test specimens were punched out from the compression molded sheets using punching die, according to Die C-ASTM D412-92. Tensile properties were measured using an Instron 4301 tensile tester with a crosshead speed of 500 mm/min and a full scale load cell of 1 kN in accordance with ASTM D638.

Hardness of 6 mm-thick samples was measured according to ASTM D2240-9 using Zwick durometer (model D-7900) with Shore A scale at room temperature.

Measurements of oil resistance and thermal aging properties

For the oil resistance test, the specimens to be tested were immersed in a bottle containing hydraulic oil (Tellus 100, Shell, Co. Ltd., Thailand) at room temperature for 70 h. Thereafter, the specimens were removed from the oil and quickly dipped in acetone and blotted lightly with filter paper to eliminate the excess oil on the specimen surfaces. Finally, tensile properties and hardness of the specimens were measured. Changes in tensile properties and hardness of specimens after oil immersion were used to determine the oil resistance.

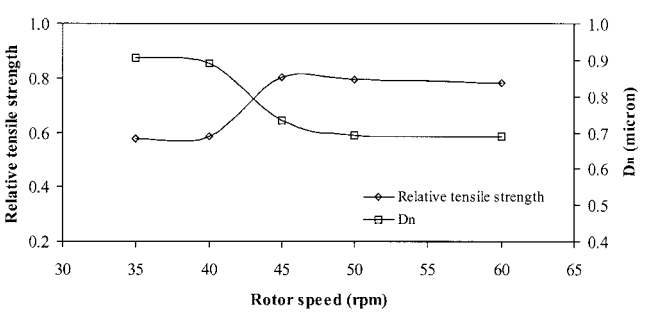

Figure 3 Relationships among relative tensile strength, rotor speed, and dispersed phase size of blends after oil immersion.

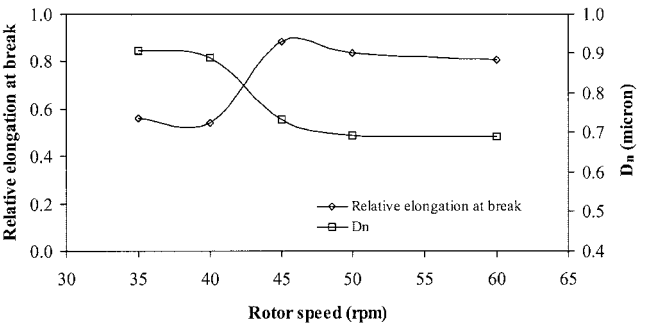

Figure 4 Relationship among relative elongation at break, rotor speed, and dispersed phase size after oil immersion.

For the determination of thermal aging properties, the specimens were placed in an oven equipped with air circulating system at the test temperature of 100°C for 24 h, according to ASTM D573. The aged specimens were then measured for tensile properties and hardness. Similar to the measurement of oil resistance, the changes in tensile strength and hardness of specimens after thermal aging were used to determine thermal aging resistance.

Blend morphology examination

Scanning electron microscopy (SEM) was performed by a JEOL scanning electron microscope, model 5800LV. The sample was stained by Osmium tetroxide (OsO_4) and sputtered with gold before viewing.

RESULTS AND DISCUSSION

Effect of rotor speed

Phase morphology

In these experiments, the temperature of mixing and the total time of mixing are 140°C and 5 min, respectively, which is based on the conditions used in the previous work.[4] The phase morphology of the blends

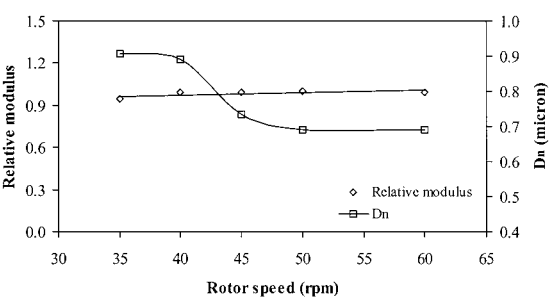

Figure 5 Relationships among relative modulus, rotor speed, and dispersed phase size after oil immersion.

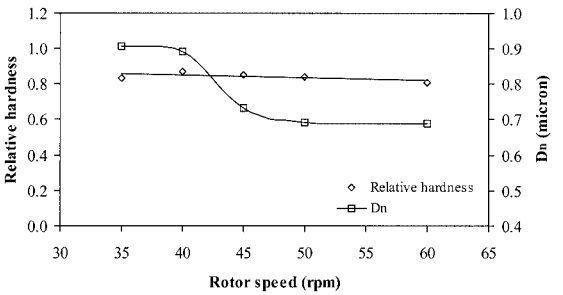

Figure 6 Relationships among relative hardness, rotor speed, and dispersed phase after oil immersion.

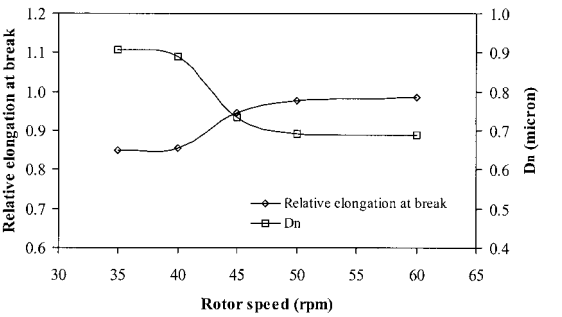

Figure 8 Relationships among relative elongation at break, rotor speed, and dispersed phase size after thermal aging.

as a function of rotor speed is given in Figures 1(a)–e) for 35, 40, 45, 50, and 60 rpm, respectively. To determine the particle size of the dispersed phase, the number-average diameter (D_n) was calculated using the image analyzing technique, and the results obtained are shown in Figure 2. At slow rotor speed [Fig. 1(a) and (b)], relatively large and nearly spherical particles of the minor NR phase dispersed in the CPE matrix are observed. As rotor speed increases, the large particles are broken down into small sizes. Similar observations are reported by Narh et al. for LCP/PET blends.[39] The results shown in Figure 2 illustrate that the most significant breakdown of the dispersed phase takes place by increasing the rotor speed from 40 to 45 rpm. The results can be explained based on Taylor's equation for Newtonian drops in a simple shear flow as shown in eq. (1).

$$d = \frac{4\gamma(\lambda + 1)}{G\eta_m\left(\frac{19\lambda}{4} + 4\right)}; \quad \lambda < 2.5 \qquad (1)$$

where G is the shear rate, d is the particle diameter, γ is the interfacial tension, and λ is the viscosity ratio $= \eta_d/\eta_m$ (η_d is the dispersed phase viscosity and η_m is the matrix phase viscosity). Taylor's equation indicates that the size of dispersed phase can be decreased by continually increasing the shear rate. However, an increase in rotor speed from 45 to 60 rpm does not have any major influence on the dispersed phase size although the particle size decreases marginally, that is, there is a minimum dispersed phase size as the shear rate is increased. The reason that the Taylor's theory is not fully applicable to the results is believed to be caused by the discontinuity of shear stress and shear rate at the interface of the immiscible binary blend leading to the poor stress transfer across the boundary phase.[32,35] In addition, an increase in the bulk temperature due to shear heating generated as a function of the rotor speed, leading to a decrease in shear stress available for disrupting the dispersed phase is probably responsible for the unchanged in phase size of the blends. The insensitivity of the phase size to a change in rotor speed was in agreement with previous work.[32,39]

Oil resistance

In this section, the relationship between rotor speed and the resistance to oil of the blends was investigated. As mentioned previously,[41] to eliminate the mastication effect as a function of rotor speed, the relative properties (tensile strength, elongation at break, modulus, and hardness), which are calculated from the ratios of these properties of the specimens after oil immersion to those before oil immersion, have been used as indicators for determining oil resistance.

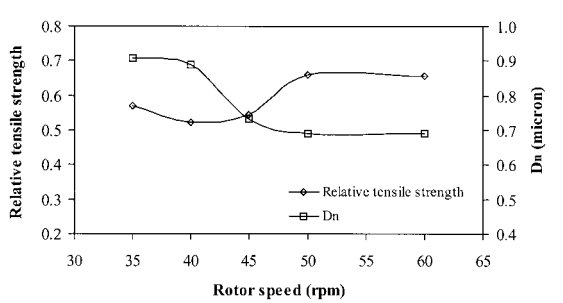

Figure 7 Relationships among relative tensile strength, rotor speed, and dispersed phase size after thermal aging.

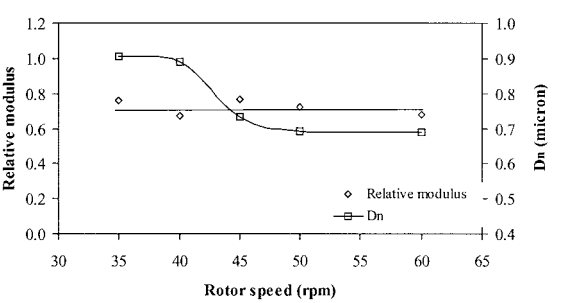

Figure 9 Relationships among relative modulus, rotor speed, and dispersed phase size after thermal aging.

Thus, the result of relative properties is mainly controlled by phase morphology of the blends.

Figures 3 to 6 show relative properties of blends prepared from various rotor speeds from 35 to 60 rpm. Figures 3 and 4 reveal that the relative tensile strength and relative elongation at break sharply increase when rotor speed is increased from 40 to 45 rpm and then level off. The results are in good agreement with the morphological results, that is, the smaller the phase size, the higher the oil resistance. Additionally, the results confirm the proposed model discussed in previous work[41] that the small phase size of nonpolar rubber in polar matrix would give the higher oil resistance of the blends.

The relative modulus at 100% strain and relative hardness of blend with different rotor speeds are shown in Figures 5 and 6. It is clear that the change in rotor speed is not found to markedly affect the relative modulus and relative hardness. In other words, only the relative tensile strength and relative elongation at break are sensitive to the change in phase morphology controlled by rotor speed. The proposed explanation is based on the difference in degree of deformation. Compared to modulus and hardness, tensile strength and elongation at break are subject to far higher deformation and therefore are more sensitive to morphological change.

Thermal aging properties

After thermal aging at 100°C for 24 h, tensile properties and hardness of the specimens were measured, and the relative properties, which are the ratios of properties after thermal aging to those before thermal aging, were used as indicators for determining thermal aging resistance. The higher the relative properties, the higher the thermal aging resistance. Figures 7 to 10 show the relative properties of thermal aging prepared from various rotor speeds. It is evident that the relative tensile strength and relative elongation at break of thermal aging shown in Figures 7 and 8 reveal similar trends to those obtained from oil resistance test. The result can be explained by the morphological change as a function of rotor speed. Similar to the oil resistance test, the change in rotor speed is not found to influence markedly the relative modulus at 100% strain and relative hardness as illustrated in Figures 9 and 10. Thus, the similar explanation can be applied.

From the results obtained, It can be seen that the morphological results agree well with the relative tensile strength and relative elongation at break for both oil resistance and thermal aging tests, that is, the smaller the dispersed phase size, the higher the oil resistance and the thermal aging properties.

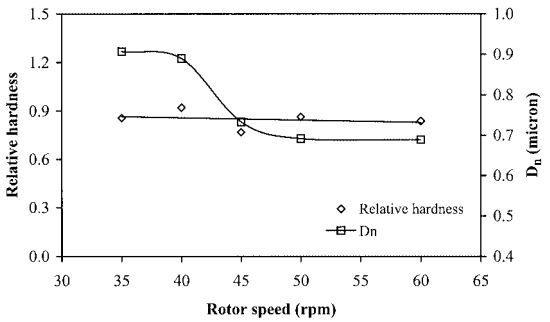

Figure 10 Relationships among relative hardness, rotor speed, and dispersed phase size after thermal aging.

Effect of mixing time

Phase morphology

To investigate the morphology development as a function of mixing time, the rotor speed and the mixing temperature were kept constant at 40 rpm and 140°C, respectively. Figure 11(a)–(e) shows the phase morphology of the 50/50 blends CPE/NR mixed for 5, 7, 10, 13, and 15 min, respectively. The number-average domain diameter as a function of mixing time is given in Figure 12.

The results indicate that, at the mixing time of 5 min, large particles of NR are dispersed in the CPE matrix. With increasing mixing time, the average size of the particles decreases and the smallest particle size are obtained at the mixing time of 10 min. The dominating process is the droplet breakage, which is attributed to the increase in total shear strain applied to the compounds. At a given shear rate, the longer blending time gives a larger total shear strain and thus a smaller dispersed phase size.[5,32 35,39] However, it is also obvious that the particle size does not decrease continuously, but reaches a minimum and, after 10 min, an increase in phase size can be observed (see Fig. 12). The possible explanation is that the excessive energy might promote the collision of the unstabilized dispersed phase, transforming them into larger domains, or the so-called phase coalescence.[5,32,38,41]

Oil resistance

Figure 13 reveals the relationship between the relative tensile strength and mixing time. It is clear that the relative tensile strength increases with increasing mixing time up to 10 mins and then decreases with further increasing mixing time. Obviously, the results of relative tensile strength and morphology are in good agreement, which support the result discussed earlier that the oil resistance of CPE/NR compounds is controlled by the size of the NR dispersed phase. It is clear from Figure 14 that the result of relative elongation at break also shows a similar trend to that of the tensile

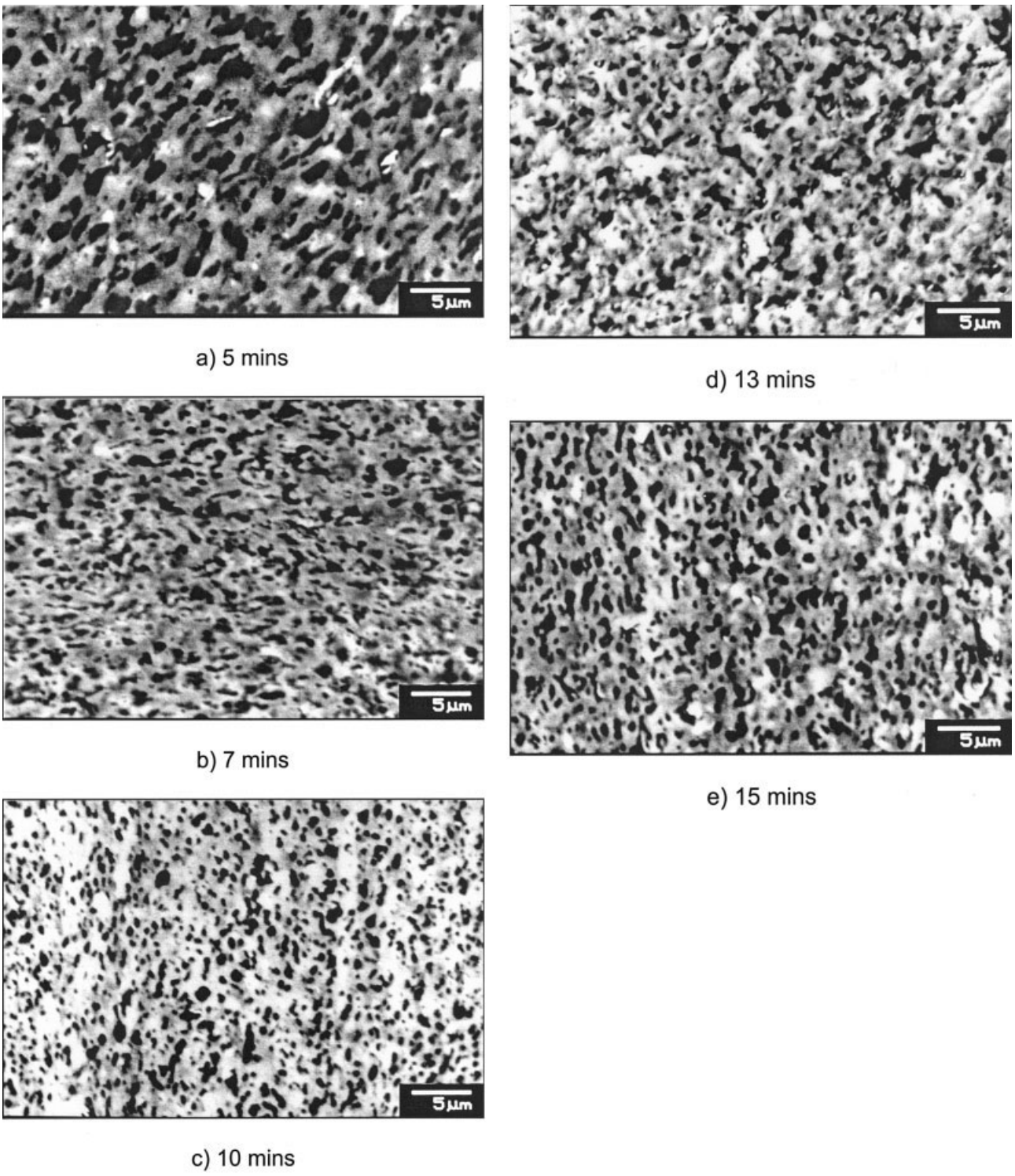

Figure 11 Scanning electron micrographs of CPE/NR blend with various mixing times: (a) 5 min; (b) 7 min; (c) 10 min; (d) 13 min; (e) 15 min.

strength. The explanation based on morphology as mentioned previously could be applied, that is, the smaller the dispersed phase size, the higher the oil resistance.

Similar to rotor speed, mixing time is not found to affect markedly the relative modulus at 100% strain and relative hardness as illustrated in Figures 15 and 16. Therefore, the similar explanation can be applied, that is, there is relatively low deformation in modulus and hardness measurements, compared to the large deformation in tensile strength and elongation at break.

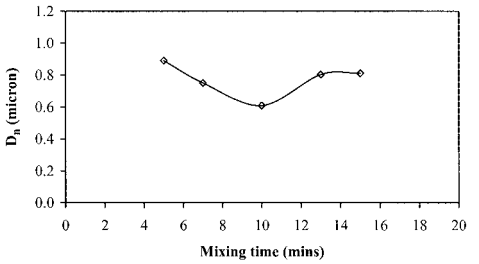

Figure 12 Relationship between dispersed phase size and mixing time.

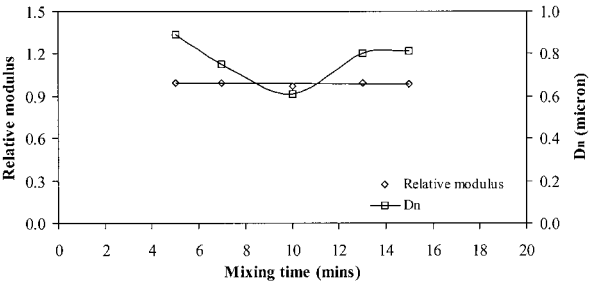

Figure 15 Relationships among relative modulus, mixing time, and dispersed phase size after oil immersion.

Thermal aging properties

The plot of mixing time and relative tensile strength of thermal aging is shown in Figure 17. It can be seen that the relative tensile strength of blend increases when mixing time increases from 5 to 10 min, and then gradually decreases. This result is correlated with morphology of blend, that is, the smallest size of the dispersed phase is obtained at the mixing time of 10 min. The plot of relative elongation at break against mixing time of CPE/NR is shown in Figure 18. The relative elongation at break result is in similar trend to relative tensile strength. It is evident that the dependence of phase size on mixing time is in good agreement with the relative properties of thermal aging resistance, that is, the smaller the dispersed phase size, the better the thermal aging properties. The relative modulus and the relative hardness of blend with different mixing times are shown in Figures 19 and 20. It can be seen that the relative modulus and the relative hardness do not depend significantly on mixing time of CPE/NR blends. The explanation is again based on the difference in degree of deformation as mentioned previously.

CONCLUSIONS

The CPE/NR blends with blend ratio of 50/50% by weight were prepared with various blending conditions. The resistance to oil and thermal aging of the blends was investigated and correlated with phase

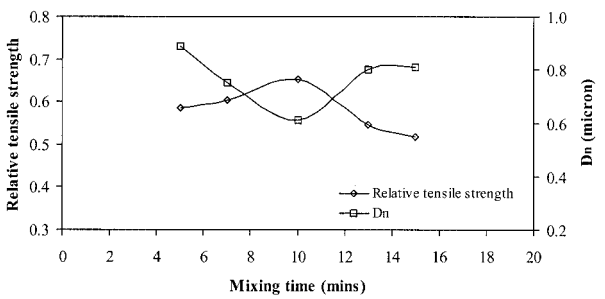

Figure 13 Relationships among relative tensile strength, mixing time, and dispersed phase size after oil immersion.

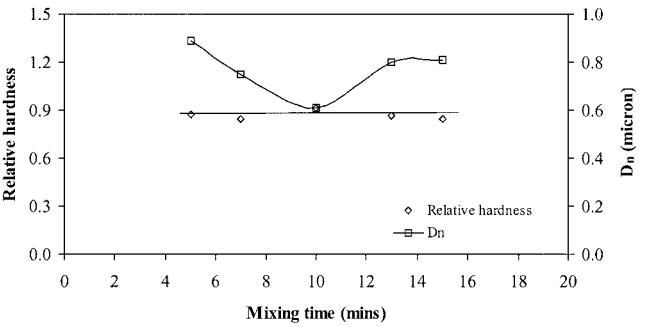

Figure 16 Relationships among relative hardness, mixing time, and dispersed phase size after oil immersion.

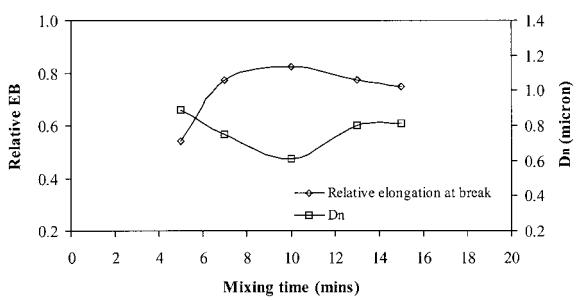

Figure 14 Relationships among relative elongation at break, mixing time, and dispersed phase size after oil immersion.

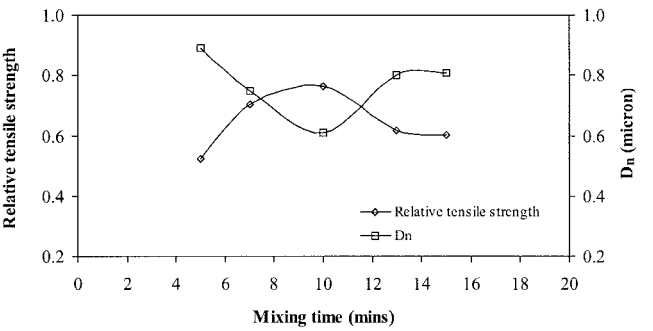

Figure 17 Relationships among relative tensile strength, mixing time, and dispersed phase size after thermal aging.

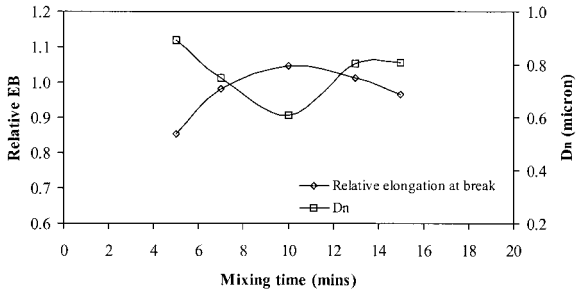

Figure 18 Relationships among relative elongation at break, mixing time, and dispersed phase size after thermal aging.

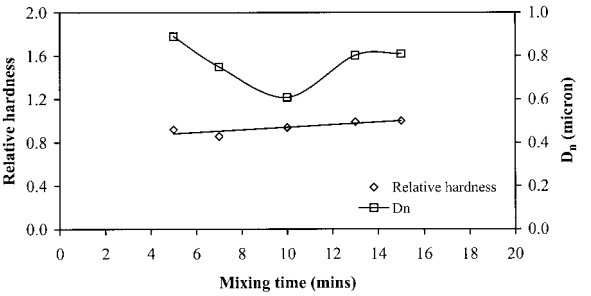

Figure 20 Relationships among relative hardness, mixing time. and dispersed phase size after thermal aging.

morphology. The following conclusions have been drawn:

1. The NR dispersed phase size in blends decreases with increasing rotor speed up to 45 rpm. It can be explained based on Taylor s equation, indicating that the phase size is inversely proportional to the shear rate. However, the NR dispersed phase size remains constant with increasing rotor speed from 45 to 60 rpm, which is probably caused by a decrease in mastication efficiency caused by shear heating.
2. With increasing mixing time, NR dispersed phase size decreases to a minimum and increases again with a further increase in mixing time. The decrease in domain size caused by domain breakup is attributed to the increase in total shear strain applied to the compounds. The increase in the phase size of the dispersed phase with a mixing time longer than 10 min is probably a result of the collision of the unstabilised dispersed phase as the mixing time is excessive.
3. The results of oil resistance and thermal aging properties are in good agreement with the morphological results, indicating that the oil resistance and thermal aging properties based on relative tensile strength in the 50/50 CPE/NR blends are controlled strongly by the size of the NR dispersed phase. The smaller the dispersed phase size, the higher the oil resistance and the thermal aging properties.

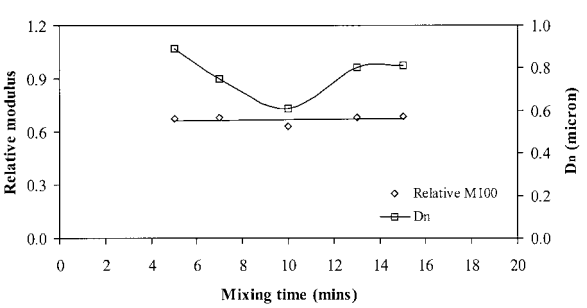

Figure 19 Relationships among relative modulus, mixing time, and dispersed phase size after thermal aging.

References

1. Utracki, L. A. Polymer Alloy and Blends: Thermodynamics and Rheology; Hanser: Munich, 1989.
2. Folkes, M. J.; Hope, P. S. Polymer Blends and Alloys; Chapman & Hall; London, 1993, 1st ed.
3. Farber, M. Rubber World 1990, 202, 19.
4. Sirisinha, C.; Sae-oui, P.; Guaysomboon, J. J Appl Polym Sci 2002, 84, 22.
5. Thomas, S.; Groeninckx, G. J Appl Polym Sci 1999, 1, 1405.
6. George, S.; Neelakantan, N. R.; Varughese, K. T.; Thomas, S. J Polym Sci Polym Phys Ed 1997, 35, 2309.
7. George, S.; Reethamma, J.; Thomas, S.; Varughese, K. T. Polymer 1995, 36, 4405.
8. George, J.; Reethamma, J.; Thomas, S.; Varughese, KT. J Appl Polym Sci 57, 1995, 449.
9. Sundararaj, U.; Macosko, C.W. Macromolecules 1995, 28, 2647.
10. Dao, K. C. Polymer 1984, 25, 1527.
11. Favis, B. D.; Therrien, D. Polymer 1991, 32, 1474.
12. Favis, B. D.; Chalifoux, J. P. Polymer 1988, 29, 1761.
13. Kumar, C. R.; George, K. E.; Thomas, S. J Appl Polym Sci 1996, 61, 2383.
14. Qin, C.; Yin, J.; Huang, B. Rubber Chem Technol 1990, 63, 77.
15. Varghese, H.; Bhagawan, S. S.; Thomas, S. J Appl Polym Sci 1999, 71, 2335.
16. Akhtar, S.; Bhagawan, S. S. Rubber Chem Technol 1987, 60, 591.
17. Tinker, A. J. Blends of Natural Rubber; Chapman & Hall: London, 1998.
18. Cimmino, S.; Dorazio, L.; Greco, R.; Maglio, G.; Malinconico, M.; Mancarella, C. Polym Eng Sci 1984, 24, 48.
19. Willis, J. M.; Favis, B. D. Polym Eng Sci 1988, 28, 1416.
20. Wu, S. Polym Eng Sci 1987, 27, 335.
21. Tang, T.; Huang, B. Polymer 1994, 35, 281.
22. Liu, Z.; Zhu, X.; Wu, L.; Li, Y.; Qi, Z.; Choy, C.; Wang, F. Polymer 2001, 42, 737.
23. Hamed, G. R. Rubber Chem Technol 1982, 55, 151.
24. Cheremisinoff, N. P. Handbook of Polymer Science and Technology: Volume 4, Composite and Specialty Applications; Marcel Dekker: New York, 1989, 1st ed.
25. Avgeropoulos, G. N.; Weissert, F. C.; Biddison, P. H.; Bohm, G. A. Rubber Chem Technol 1976, 49, 93.

26. Karger-Kocsis, J.; Kallo, A.; Kuleznev, V. N. Polymer 1984, 25, 279.
27. Sirisinha, C.; Baulek-Limcharoen, S.; Thunyarittikorn, J. Plast Rubber Compos Process Appl 2001, 30, 314.
28. Wildes, G.; Keskkula, H.; Paul, D. R. J Polym Sci Polym Phys Ed 1999, 37, 71.
29. Favis, B. D.; Chalifoux, J. P. Polym Eng Sci 1987, 27, 1591.
30. Valsamis, L. N.; Kearney, M. R.; Dagli, S. S.; Merhta, D. D.; Polchocki, A. P. Adv Polym Technol 1988, 8, 115.
31. Pukanszky, B.; Fortelny, I.; Kovar, J.; Tudos, F. Plast Rubber Compos Proc Appl 1991, 15, 31.
32. Favis, B. D. J Appl Polym Sci 1990, 39, 285.
33. Chaudhry, B. I.; Hage, E.; Pessan, L. A. J Appl Polym Sci 1998, 67, 1605.
34. Bu, W.; He, J. J Appl Polym Sci 1996, 62, 1445.
35. Yang, L. Y.; Bigio, D.; Smith, T. G. J Appl Polym Sci 1995, 58, 129.
36. Tokita, N. Rubber Chem Technol 1977, 50, 292.
37. Ishiaku, U. S.; Ismail, H.; Ishak, Z. A. J Appl Polym Sci 1999, 73, 75.
38. Fortelny, I.; Michalkova, D. Plast Rubber Compos Proc Appl 1998, 27, 53.
39. Narh, K. A.; Zhang, Q.; Li, Z. J Appl Polym Sci 2000, 75, 1783.
40. Min, K.; White, J. L.; Fellers, J. F. J Appl Polym Sci 1984, 29, 2117.
41. Sirisinha, C.; Baulek-Limcharoen, S.; Thunyarittikorn, J. J Appl Polym Sci 2001, 82, 1232.